ACADEMIC PRESS

Available online at www.sciencedirect.com

SCIENCE DIRECT®

Journal of Sound and Vibration 264 (2003) 873–882

JOURNAL OF SOUND AND VIBRATION

www.elsevier.com/locate/jsvi

Bifurcation and chaos of a harmonically excited oscillator with both stiffness and viscous damping piecewise linearities by incremental harmonic balance method

L. Xu[a,*], M.W. Lu[a], Q. Cao[b]

[a] *Department of Engineering Mechanics, Tsinghua University, Beijing 100084, People's Republic of China*
[b] *Department of Mathematics and Physics, Shandong University, Jinan 250061, People's Republic of China*

Received 26 November 2001; accepted 5 August 2002

Abstract

In this paper, an explicit formulation of the incremental harmonic balance (IHB) scheme for computation of periodic solutions of a harmonically excited oscillator which is asymmetric with both stiffness and viscous damping piecewise linearities is derived. Analysis of dynamical behavior as bifurcation and chaos of the non-linear vibration system considered is effectively carried out by the IHB procedure, showing that the system exhibits chaos via the route of period-doubling bifurcation, with coexistence of multiple periodic attractors observed and analyzed by the interpolated cell mapping method. In addition, numerical simulation by the IHB method is compared with that by the fourth order Runge–Kutta numerical integration routine, which shows that this method is in many respects distinctively advantageous over classical approaches, and especially excels in performing parametric studies.

1. Introduction

In mechanical vibrating systems like lightly loaded spur gears, rotor systems, relaxation oscillator systems, cam/follower systems, linkage joints and robotic components, bearings and impact print hammers, piecewise linearity or piecewise-non-linearity exists due to clearances, gaps, backlash and impacting components, etc. In other fields of electronics, biology, economy, the theoretical models of many non-linear dynamical problems are also found to be systems having piecewise features [1–4].

*Corresponding author.
E-mail address: xulei00@mails.tsinghua.edu.cn (L. Xu).

0022-460X/03/$ - see front matter
PII: S0022-460X(02)01194-X

As revealed by the motion of a mooring tower with bilinear stiffness characteristics of the mooring line studied by Thompson, systems with a piecewise linearity may exhibit very complex dynamical behavior [5,6]. Some higher dimensional piecewise-linear circuits have even been found to display hyperchaos [7,8]. Though it is well known that the free vibrations of piecewise-linear dynamical systems can be solved exactly by gluing together the solutions in each linear zone, it is not yet feasible to obtain a closed-form solution for an excited steady state vibration. Classical perturbation methods such as Lindstedt–Poincare, Krylov–Bogoliubov–Mitropolsky, or multiple scale method [9] are valid only when the non-linearity of the considered dynamical system is weak. Though the harmonic balance method can deal with systems with strong non-linearity, the scheme must be reformulated when more harmonic terms are taken in order to get more accurate periodic solutions. Other numerical approaches like the fourth order Runge–Kutta integration method are usually time consuming when performing parametric studies, especially when the rate of convergence is very low.

Based on an incremental Hamilton's principle, a versatile and systematic computer implementation for treating periodic structural vibrations of elastic systems was developed by Cheung and Lau [10]. Compared with classical approaches, the incremental harmonic balance (IHB) method is not confined to small exciting parameters and weak non-linearity, and is remarkably effective in computer implementation for obtaining response with a desired accuracy over a wide range of varying parameter, with both stable and unstable solutions, subharmonic, harmonic and superharmonic resonances being traced directly. Ever since its derivation, the IHB method has found application in a wide range of dynamical systems. In Ref. [11], solution diagrams of van der Pol oscillator are plotted using this method. In Refs. [12,13], the method is applied, respectively, to the analysis of bifurcation and chaos of an escape equation model and an articulated loading platform with piecewise-non-linear stiffness. In Ref. [14], by expansion of the sign non-linearity for small increments, the IHB method is modified to perform a multi-harmonic frequency-domain analysis of dry friction damped systems. In Ref. [15], periodic limit cycles of a non-linear oscillator subjected to periodic excitation are analyzed where the stiffness of the system is of unsymmetrical piecewise linearity. In Ref. [16], the IHB method is further extended to the periodic vibrations of non-linear systems with a general form of piecewise-linear restoring force, which is of great significance as many structural and mechanical systems of practical interest possess a piecewise-linear stiffness.

In this paper, the IHB computation scheme is derived for a class of single-degree-of-freedom (d.o.f.) systems with coexistence of stiffness and viscous damping piecewise linearities, showing great accuracy compared with the result of direct numeric integration method. As many systems possess both stiffness and damping non-linearities, the formulation in the paper can readily be applied to the analysis of complex dynamical behaviors as bifurcation and chaos of such systems in engineering practice.

2. Piecewise-linear dynamical system

The non-linear oscillator considered here is a single-d.o.f. vibration system as shown in Fig. 1, with both stiffness and viscous damping piecewise linearities, which serves as the model for a wide range of piecewise-linear vibration systems in engineering practice. Complex dynamical properties

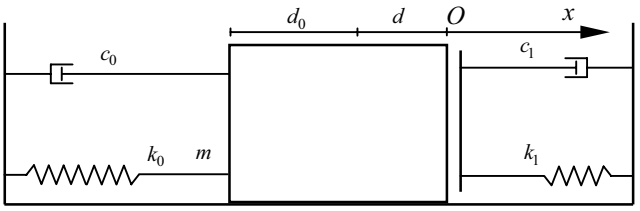

Fig. 1. Dynamic oscillator with both stiffness and viscous damping piecewise linearities.

such as the static bifurcation and periodic-doubling bifurcation to chaos of the system have been studied in Ref. [17] by the theory of singularity, Runge–Kutta numerical integration method and Poincare map.

Suppose that without the mass m, the two free springs would just touch each other. For the damper and the linear spring which are at the left side of the mass and connected to it, and those at the right side and not connected to it, their respective damping or stiffness are denoted by c_0, k_0, c_1, k_1. Assume that when the oscillator is at the state of static equilibrium, d_0, d, respectively, denote the compression of the spring at both sides and thus $k_0 d_0 = k_1 d$. Let the displacement x denote the co-ordinate of the right edge of the mass relative to the fixed point O, which itself is the position of the right edge at static equilibrium, the system is represented by the following control equation:

$$m\frac{\mathrm{d}^2x}{\mathrm{d}t^2} + h\left(\frac{\mathrm{d}x}{\mathrm{d}t}\right) + g(x) = f_0 \sin \omega t, \tag{1}$$

$$h\left(\frac{\mathrm{d}x}{\mathrm{d}t}\right) = \begin{cases} (c_0 + c_1)\dfrac{\mathrm{d}x}{\mathrm{d}t}, & x > -d, \\ c_0\dfrac{\mathrm{d}x}{\mathrm{d}t}, & x \leqslant -d, \end{cases} \quad g(x) = \begin{cases} (k_0 + k_1)x, & x > -d, \\ k_0(x - d_0), & x \leqslant -d. \end{cases}$$

For convenience, the piecewise-linear viscous damping force $h(\mathrm{d}x/\mathrm{d}t)$ and the restoring force $g(x)$ are reformulated as the following form:

$$h\left(\frac{\mathrm{d}x}{\mathrm{d}t}\right) = c_0\left[\frac{\mathrm{d}x}{\mathrm{d}t} + H\left(\frac{\mathrm{d}x}{\mathrm{d}t}\right)\right], \quad g(x) = k_0 x + G(x), \tag{2}$$

$$H\left(\frac{\mathrm{d}x}{\mathrm{d}t}\right) = \begin{cases} \dfrac{c_1}{c_0}\dfrac{\mathrm{d}x}{\mathrm{d}t}, & x > -d, \\ 0, & x \leqslant -d, \end{cases} \quad G(x) = \begin{cases} k_1 x, & x > -d, \\ -k_1 d, & x \leqslant -d. \end{cases}$$

By letting a new time scale $\tau = \omega t$, frequency ratio $\Omega = (\omega/\sqrt{k_0/m})$, damping ratio $\zeta = (c_0/2\sqrt{mk_0})$, and noting that the piecewise-linear function $H(\mathrm{d}x/\mathrm{d}t)$ is homogeneous with respect to $\mathrm{d}x/\mathrm{d}t$, thus $H(\omega \mathrm{d}x/\mathrm{d}\tau) = \omega H(\mathrm{d}x/\mathrm{d}\tau)$, Eq. (1) is transformed into

$$\Omega^2\frac{\mathrm{d}^2x}{\mathrm{d}\tau^2} + 2\zeta\Omega\frac{\mathrm{d}x}{\mathrm{d}\tau} + x + 2\zeta\Omega H\left(\frac{\mathrm{d}x}{\mathrm{d}\tau}\right) + \frac{1}{k_0}G(x) = \frac{1}{k_0}f_0 \sin \tau. \tag{3}$$

It is obvious that when the peak amplitude of the steady periodic solution of Eq. (3) is less than d, the linear springs at both sides will function simultaneously thus system (3) equals to a linear system. Only when the peak amplitude is larger than d, can Eq. (3) exhibit complex dynamical behavior characteristic of non-linear systems.

3. IHB scheme of the piecewise-linear system

With regard to the piecewise-linear differential system (3), by a Newton–Raphson procedure, assume that $x_0(\tau)$ stands for an initially approximated vibrating state corresponding to the excitation parameters Ω_0 and the excitation level f_0 is fixed, a neighboring state may be denoted by

$$x(\tau) = x_0(\tau) + \Delta x(\tau), \quad \Omega = \Omega_0 + \Delta\Omega, \tag{4}$$

where $\Delta x(\tau)$ and $\Delta\Omega$ are small increments.

Correspondingly, the piecewise-linear function $H(\mathrm{d}x/\mathrm{d}\tau)$ and $G(x)$ may be expressed by a first order Taylor expansion as

$$H\left(\frac{\mathrm{d}x}{\mathrm{d}\tau}\right) = H\left(\frac{\mathrm{d}x_0}{\mathrm{d}\tau}\right) + H'\left(\frac{\mathrm{d}x_0}{\mathrm{d}\tau}\right)\frac{\mathrm{d}\Delta x}{\mathrm{d}\tau}, \quad G(x) = G(x_0) + G'(x_0)\,\Delta x, \tag{5}$$

where

$$H'\left(\frac{\mathrm{d}x_0}{\mathrm{d}\tau}\right) = \begin{cases} \dfrac{c_1}{c_0}, & x_0 > -d, \\ 0, & x_0 \leqslant -d, \end{cases} \quad G'(x_0) = \begin{cases} k_1, & x_0 > -d, \\ 0, & x_0 \leqslant -d. \end{cases}$$

By substituting expressions (4), (5) into Eq. (3) and neglecting the non-linear terms of the small increments, Eq. (3) becomes linearized as

$$\Omega_0^2\frac{d^2\Delta x}{\mathrm{d}\tau^2} + 2\zeta\Omega_0\frac{\mathrm{d}\Delta x}{\mathrm{d}\tau} + \Delta x + 2\zeta\Omega_0 H'\left(\frac{\mathrm{d}x_0}{\mathrm{d}\tau}\right)\frac{\mathrm{d}\Delta x}{\mathrm{d}\tau} + \frac{1}{k_0}G'(x_0)\Delta x = \bar{R} + \Delta\Omega\bar{S}, \tag{6}$$

where

$$\bar{R} = -\left[\Omega_0^2\frac{\mathrm{d}^2x_0}{\mathrm{d}\tau^2} + 2\zeta\Omega_0\frac{\mathrm{d}x_0}{\mathrm{d}\tau} + x_0 + 2\zeta\Omega_0 H\left(\frac{\mathrm{d}x_0}{\mathrm{d}\tau}\right) + \frac{1}{k_0}G(x_0) - \frac{1}{k_0}f_0\sin\tau\right],$$

$$\bar{S} = -2\Omega_0\frac{\mathrm{d}^2x_0}{\mathrm{d}\tau^2} - 2\zeta\frac{\mathrm{d}x_0}{\mathrm{d}\tau} - 2\zeta H\left(\frac{\mathrm{d}x_0}{\mathrm{d}\tau}\right), \tag{7}$$

where $\bar{R}$ is the corrective term which goes to zero when the solution is reached.

Though Eq. (6) is linear, there are variable coefficients due to piecewise linearity of the damping force and restoring force, thus it does not seem feasible to solve directly, hence a Galerkin procedure is carried out as follows. Both the approximate initial periodic solution and its small increment may be expressed as

$$x_0 = \frac{a_0}{2} + \sum_{n=1}^{N}(a_n\cos n\tau + b_n\sin n\tau), \quad \Delta x = \frac{\Delta a_0}{2} + \sum_{n=1}^{N}(\Delta a_n\cos n\tau + \Delta b_n\sin n\tau), \tag{8}$$

where N is the number of harmonic terms taken in the limited Fourier series. By taking Δa_n's, Δb_n's as the generalized co-ordinates, it is derived from Eq. (6) that

$$\int_0^{2\pi}\left[\Omega_0^2\frac{\mathrm{d}^2\Delta x}{\mathrm{d}\tau^2}+2\zeta\Omega_0\frac{\mathrm{d}\Delta x}{\mathrm{d}\tau}+\Delta x+2\zeta\Omega_0 H'\left(\frac{\mathrm{d}x_0}{\mathrm{d}\tau}\right)\frac{\mathrm{d}\Delta x}{\mathrm{d}\tau}+\frac{1}{k_0}G'(x_0)\Delta x\right]\delta(\Delta x)\,\mathrm{d}\tau$$
$$=\int_0^{2\pi}\left(\bar{R}+\Delta\Omega\bar{S}\right)\delta(\Delta x)\,\mathrm{d}\tau, \tag{9}$$

which is equivalent to a system of $2N+1$ linearized equations with the Δa_n's and Δb_n's being variables

$$C\Delta a=R+\Delta\Omega S, \tag{10}$$

where

$$a=[a_0,a_1,\ldots,a_N,b_1,b_2,\ldots,b_N]^{\mathrm{T}},\quad \Delta a=[\Delta a_0,\Delta a_1,\ldots,\Delta a_N,\Delta b_1,\Delta b_2,\ldots,\Delta b_N]^{\mathrm{T}},$$

$$C=\begin{bmatrix}C_{11}^L+C_{11}^{NL} & C_{12}^L+C_{12}^{NL}\\ C_{21}^L+C_{21}^{NL} & C_{22}^L+C_{22}^{NL}\end{bmatrix},\quad R=\begin{bmatrix}R_1^L+R_1^{NL}\\ R_2^L+R_2^{NL}\end{bmatrix},\quad S=\begin{bmatrix}S_1^L+S_1^{NL}\\ S_2^L+S_2^{NL}\end{bmatrix}. \tag{11}$$

The explicit expressions for the linear elements of the above matrices C, R, and S are worked out the same as in Ref. [16], while in this case, the matrix S contains both linear and non-linear parts due to the piecewise-linear damping force

$$\begin{aligned}
&C_{11ij}^L=\alpha_j\delta_{ij}\pi(1-j^2\Omega_0^2)\quad(i=0,1,\ldots,N;\ j=0,1,\ldots,N),\\
&C_{12ij}^L=2j\delta_{ij}\pi\zeta\Omega_0\quad(i=0,1,\ldots,N;\ j=1,\ldots,N),\\
&C_{21ij}^L=-2j\delta_{ij}\pi\zeta\Omega_0\quad(i=1,2,\ldots,N;\ j=0,1,\ldots,N),\\
&C_{22ij}^L=\delta_{ij}\pi(1-j^2\Omega_0^2)\quad(i=1,2,\ldots,N;\ j=1,\ldots,N),\\
&R_{1i}^L=-\alpha_i\left[(1-i^2\Omega_0^2)a_i+2i\zeta\Omega_0 b_i\right]\pi\quad(i=0,1,\ldots,N),\\
&R_{2i}^L=-\left[(1-i^2\Omega_0^2)b_i-2i\zeta\Omega_0 a_i-\frac{f_0}{k_0}\right]\pi\quad(i=1),\\
&R_{2i}^L=-\left[(1-i^2\Omega_0^2)b_i-2i\zeta\Omega_0 a_i\right]\pi\quad(i=2,\ldots,N),\\
&S_{1i}^L=2\pi i(i\Omega_0 a_i-\zeta b_i)\quad(i=0,1,\ldots,N),\\
&S_{2i}^L=2\pi i(i\Omega_0 b_i+\zeta a_i)\quad(i=0,1,\ldots,N),
\end{aligned} \tag{12}$$

where

$$\delta_{ij}=\begin{cases}1, & i=j,\\ 0, & i\neq j,\end{cases}\qquad \alpha_n=\begin{cases}1, & n=0,\\ 1/2, & n\neq 0.\end{cases} \tag{13}$$

The non-linear parts in Eq. (11) are expressed by

$$
\begin{aligned}
C_{11ij}^{NL} &= -2j\alpha_i\zeta\Omega_0 \int_0^{2\pi} H'\left(\frac{\mathrm{d}x_0}{\mathrm{d}\tau}\right)\cos i\tau \sin j\tau \,\mathrm{d}\tau + \frac{\alpha_i\alpha_j}{k_0}\int_0^{2\pi} G'(x_0)\cos i\tau\cos j\tau \,\mathrm{d}\tau,\\
C_{12ij}^{NL} &= 2j\alpha_i\zeta\Omega_0 \int_0^{2\pi} H'\left(\frac{\mathrm{d}x_0}{\mathrm{d}\tau}\right)\cos i\tau \cos j\tau \,\mathrm{d}\tau + \frac{\alpha_i}{k_0}\int_0^{2\pi} G'(x_0)\cos i\tau\sin j\tau \,\mathrm{d}\tau,\\
C_{21ij}^{NL} &= -2j\zeta\Omega_0 \int_0^{2\pi} H'\left(\frac{\mathrm{d}x_0}{\mathrm{d}\tau}\right)\sin i\tau \sin j\tau \,\mathrm{d}\tau + \frac{\alpha_j}{k_0}\int_0^{2\pi} G'(x_0)\sin i\tau\cos j\tau \,\mathrm{d}\tau,\\
C_{22ij}^{NL} &= 2j\zeta\Omega_0 \int_0^{2\pi} H'\left(\frac{\mathrm{d}x_0}{\mathrm{d}\tau}\right)\sin i\tau \cos j\tau \,\mathrm{d}\tau + \frac{1}{k_0}\int_0^{2\pi} G'(x_0)\sin i\tau\sin j\tau \,\mathrm{d}\tau,\\
R_{1i}^{NL} &= -2\alpha_i\zeta\Omega_0 \int_0^{2\pi} H\left(\frac{\mathrm{d}x_0}{\mathrm{d}\tau}\right)\cos i\tau \,\mathrm{d}\tau - \frac{\alpha_i}{k_0}\int_0^{2\pi} G(x_0)\cos i\tau \,\mathrm{d}\tau,\\
R_{2i}^{NL} &= -2\zeta\Omega_0 \int_0^{2\pi} H\left(\frac{\mathrm{d}x_0}{\mathrm{d}\tau}\right)\sin i\tau \,\mathrm{d}\tau - \frac{1}{k_0}\int_0^{2\pi} G(x_0)\sin i\tau \,\mathrm{d}\tau,\\
S_{1i}^{NL} &= -2\alpha_i\zeta \int_0^{2\pi} H\left(\frac{\mathrm{d}x_0}{\mathrm{d}\tau}\right)\cos i\tau \,\mathrm{d}\tau, \quad S_{2i}^{NL} = -2\zeta\int_0^{2\pi} H\left(\frac{\mathrm{d}x_0}{\mathrm{d}\tau}\right)\sin i\tau \,\mathrm{d}\tau.
\end{aligned}
\tag{14}
$$

The evaluation of these piecewise-linear integrals in programming can be achieved explicitly by a procedure using bisection and interpolation method, which has been well expounded in Ref. [16]. The Ω-incrementation procedure for obtaining the frequency response curve of a dynamical system may be carried out by incrementing Ω from point to point, which implies that $\Delta\Omega = 0$ though the iteration process at every point, leading to the following equations:

$$
C^{(i)}\Delta a^{(i+1)} = R^{(i)}, \quad a^{(i+1)} = a^{(i)} + \Delta a^{(i+1)}. \tag{15}
$$

Being reevaluated in terms of the $(i+1)$th amplitude vector $a^{(i+1)}$, the matrices $C^{(i+1)}$, $R^{(i+1)}$ are updated at every increment.

From the derivation of the IHB computation scheme, it can be seen that N, that is, number of harmonics taken in the limited Fouries series, is incorporated into the iteration process as an independent parameter, and thus can be conveniently varied according to the required precision, facilitating programming in computer simulation.

4. Numerical simulation

As already tested and evaluated in many relevant papers, the IHB method for computing periodic solutions of non-linear dynamical systems is distinctively advantageous over classical approaches. The fundamental and superharmonic resonances are directly obtained from the Fourier expansion of $x(\tau)$. To obtain the mth order subharmonic resonances, one simply shifts the excitation force to $f_0 \sin m(\omega t)$. The amplitudes of vibration may be expressed either as peak amplitudes per cycle or as the norm of the harmonic components which is indicative of the total

energy of the motion. As to system (3), the control parameter is taken as $k = k_0 \times 10^{-3}$, where k_0 is the stiffness of the linear spring at the left side of the mass, and other parameter values are fixed as

$$f_0 = 7.8 \times 10^3, \quad m = 0.4 \times 10^3, \quad k_1 = 0.9 \times 10^6,$$
$$c_0 = 0.05 \times 10^3, \quad c_1 = 0.5 \times 10^3, \quad d = 5 \times 10^{-3}, \quad \omega = 34.56. \tag{16}$$

It is easily found that when k is very large, which means that the spring at the left side of the mass is quite rigid, the peak amplitude of the steady periodic state of the oscillator will not exceed d, thus the system equals to a linear system with period-1, corresponding to the period of the external harmonic excitation. In the following study, this trivial case will be ignored and k is designated to be relatively small, varying in the range [2,20]. By the IHB scheme (15), the peak amplitudes of the different periodic responses can be plotted as a function of the bifurcation parameter and the response diagram is shown in Fig. 2.

In Fig. 2(a), with a decreasing value of k, a double-period-2 process of the considered continuous piecewise-linear system is observed which is similar to the behavior of the well-known one-dimensional discrete system given by logistic map. Starting from point 'a' corresponding to $k = 19.5$, the system exhibits a period-2 response corresponding to the period of the external harmonic excitation until the point 'b', when $k = 5.2$. At this point the period-2 solution bifurcates to a period-4 solution through a period-doubling bifurcation confirmed by noting that the eigenvalue of the monodromy matrix moves out of the unit circle in the -1 direction. The period-4 solution further bifurcates into a period-8 solution at point 'c' when $k = 3.1$. In Fig. 2(b), a period-3 response curve is traced by the IHB scheme over the range of bifurcation parameter [2,5] in which a period-4 or 8 solution coexists as shown in Fig. 2(a). This is important in the light of the famous assertion by Li–Yorke, that is 'period-three means chaos' [18]. The initial condition map corresponding to the coexistent period-4 and period-3 solution at $k = 4.5$ is obtained by the interpolated cell mapping method [19] shown in Fig. 3. Starting from initial conditions corresponding to the blank space ends up in the period-4 attractor, while solutions starting from the shaded region result in the period-3 attractor. In the generation of the above curves, the IHB method uses an initial guess of the amplitude vector and iterates until convergence is achieved, and the following rate of convergence is then remarkably improved by choosing the initial guess

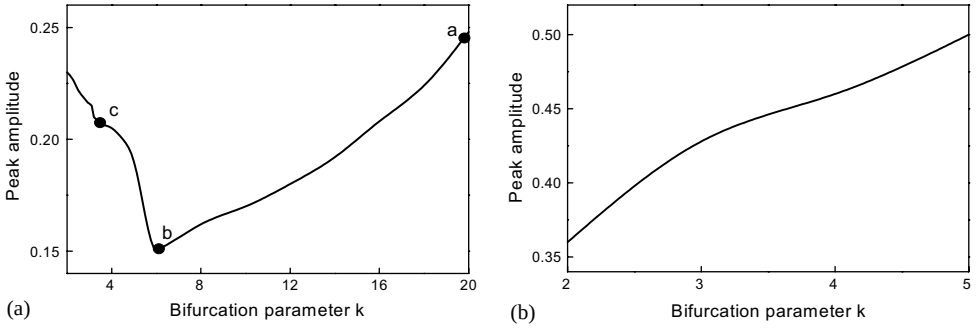

Fig. 2. Response curve of the system: (a) period-doubling bifurcation and (b) coexistence of period-3 response.

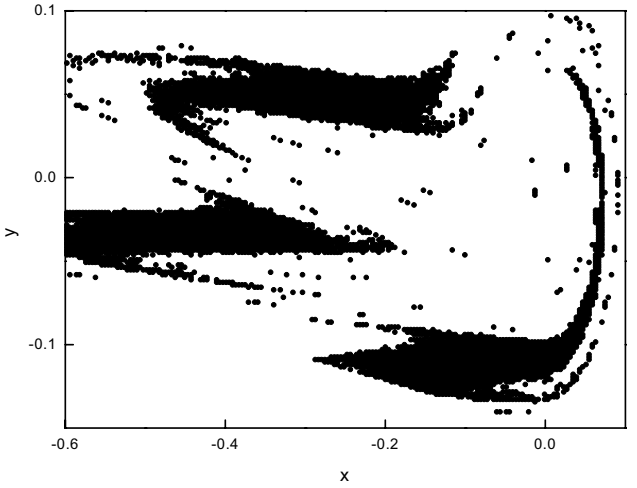

Fig. 3. Basin of attraction: white region, period-4 attractor; shaded region, period-3 attractor.

of the amplitude vector to be the already converged vector from a neighboring bifurcation parameter.

The accuracy of the IHB method is evaluated here by comparing the results against those of existing time domain analysis. In this case, a fourth order Runge–Kutta numerical integration routine is used to provide an accurate basis for comparison. The phase planes of the steady periodic responses with different period at different values of k are given in Fig. 4, where the solid lines and the discrete dotted marks respectively stand for the solutions obtained by the IHB method and the numeric integration procedure. The norm of the residue vector and increments of the Fourier coefficients in the IHB method are reduced to less than 1.0×10^{-5} in obtaining all these solutions, and it can be seen that there is an excellent fit between the IHB solutions and the numerically integrated ones. In the meanwhile, the small circles in the figures above denote the fixed points of the corresponding solutions with different period, which are obtained by the Poincaré map of the non-autonomous system (3):

$$\begin{aligned} \dot{x} &= y, \\ \dot{y} &= \left[x + \frac{1}{k_0}G(x) + 2\zeta\Omega y + 2\zeta\Omega H(\dot{y}) - \frac{1}{k_0}f_0 \sin\theta\right]/\Omega^2, \\ \dot{\theta} &= 1. \end{aligned} \tag{17}$$

It is observed that from Figs. 4(a)–(c), the fixed points undergo successive double-period-2 bifurcation from period-2 to period-8 with decreasing bifurcation parameter values.

Successive decreasing values of the bifurcation parameter k will give rise to further period-doubling bifurcation process of the system, which will at last ends up in a chaotic state as shown in Fig. 5. This typical route to chaos is well researched in the one-dimensional discrete mapping systems like the famous logistic map [20]. On the other hand, higher dimensional systems do possess dynamical properties which lower ones do not have. In the case considered, for example, coexistence of attractors as shown in Fig. 3 is denied to the logistic map.

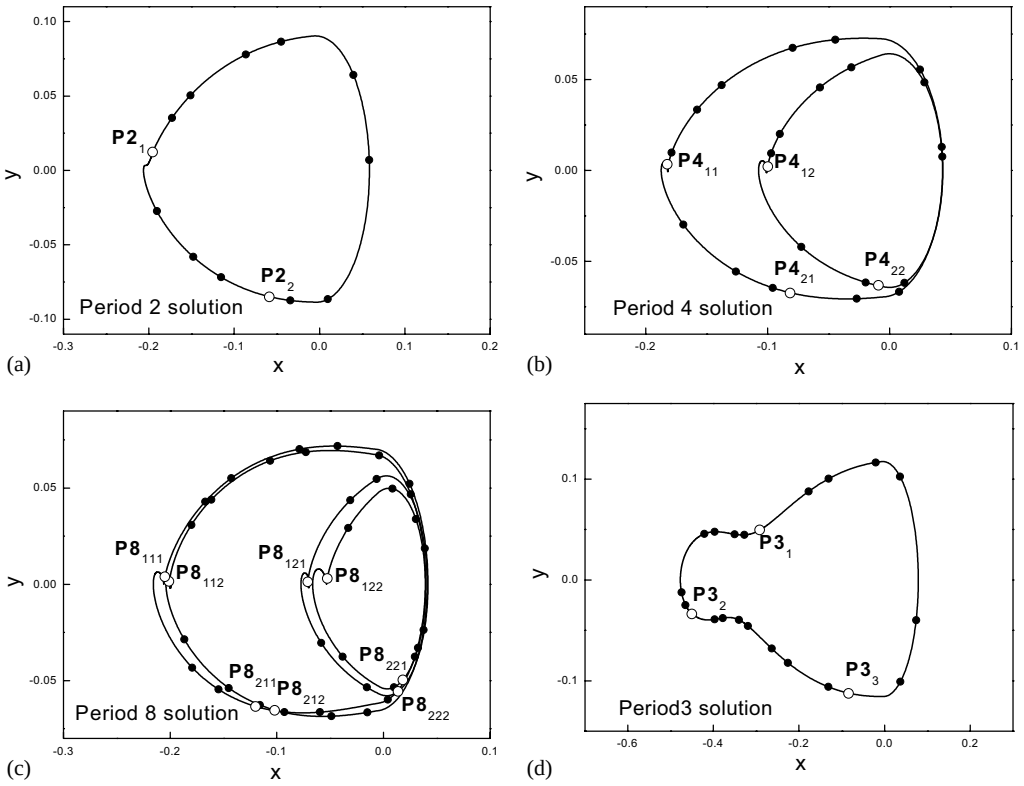

Fig. 4. Phase plane of solutions with different period by the IHB method compared with the result of numeric integration, and the corresponding fixed points by Poincaré map.

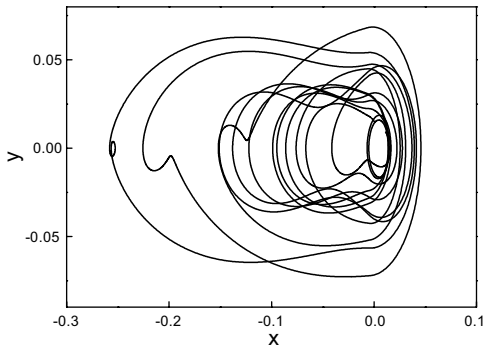

Fig. 5. Chaotic state of vibration.

5. Conclusion

In this paper, the incremental harmonic balance (IHB) method is successfully extended to a class of non-linear dynamical systems with coexistence of stiffness and viscous damping piecewise

linearity for computing periodic solutions, which is in many respects distinctively advantageous over classical approaches. Numerical simulation of the harmonically excited oscillator is effectively carried out by the IHB scheme, and the results compare very well with that by the fourth order Runge–Kutta numerical integration routine. A parametric study performed by the IHB method reveals that the system exhibit chaos via the typical route of period-doubling bifurcation similar to that of the well-known one-dimensional logistic map. In the meanwhile, the distinctive phenomenon of coexistence of multiple periodic attractors is observed and analyzed by the interpolated cell mapping method.

References

[1] S. Wiggins, Introduction to Applied Nonlinear Dynamical Systems and Chaos, Springer, New York, 1990.
[2] K. Murali, M. Lakshmanan, L.O. Chua, The simplest dissipative nonautomous chaotic circuit, IEEE Transactions on Circuits and Systems 41 (1994) 462–463.
[3] Y.S. Choi, S.T. Noah, Forced periodic vibration of unsymmetric piecewise-linear systems, Journal of Sound and Vibration 121 (1988) 117–126.
[4] S. Maezawa, H. Kumano, Y. Minakuchi, Forced vibrations in an unsymmetric piecewise-linear system excited by general periodic force functions, Bulletin of the JSME 23 (1980) 68–75.
[5] J.M. Thompson, Complex dynamics of compliant off shore structures, Proceedings of the Royal Society of London 387 (1983) 407–427.
[6] J.M. Thompson, A.R. Bokain, R. Ghaffari, Subharmonic resonances and chaotic motions of the bilinear oscillator, IMA Journal of Applied Mathematics 31 (1983) 207–234.
[7] J.L. Hudson, H.C. Killory, Chaos in a four-variable piecewise-linear system of differential equations, IEEE Transactions on Circuits and Systems 35 (1998) 902–908.
[8] T. Matsumoto, L.O. Chua, K. Kobayashi, Hyperchaos: laboratory experiment and numerical confirmation, IEEE Transactions on Circuits and Systems 33 (1986) 1143–1147.
[9] J.J. Stijer, Nonlinear Vibrations in Mechanical and Electrical Systems, Wiley, New York, 1992.
[10] S.L. Lau, Y.K. Cheung, Amplitude incremental variational principle for nonlinear vibration of elastic system, American Society of Mechanical Engineers, Journal of Applied Mechanics 48 (1981) 959–964.
[11] S.L. Lau, S.W. Yuen, Solution diagram of nonlinear dynamic systems by the IHB method, Journal of Sound and Vibration 167 (1993) 303–316.
[12] A. Raghothama, S. Narayanan, Bifurcation and chaos in escape equation model by incremental harmonic balancing, Chaos Solitons & Fractals 11 (2000) 1349–1363.
[13] A. Raghothama, S. Narayanan, Bifurcation and chaos of an articulated loading platform with piecewise non-linear stiffness using the incremental harmonic balance method, Ocean Engineering 27 (2000) 1087–1107.
[14] C. Pierre, A.A. Ferri, E.H. Dowell, Multi-harmonic analysis of dry friction damped systems using an incremental harmonic balance method, Journal of Applied Mechanics 52 (1985) 958–964.
[15] C.W. Wong, W.S. Zhang, S.L. Lau, Periodic forced vibration of unsymmetrical piecewise-linear systems by incremental harmonic balance method, Journal of Sound and Vibration 149 (1991) 91–105.
[16] S.L. Lau, W.S. Zhang, Nonlinear vibrations of piecewise-linear systems by incremental harmonic balance method, Journal of Applied Mechanics 59 (1992) 153–160.
[17] Q. Cao, L. Xu, K. Djidjeli, Analysis of period-doubling and chaos of a non-symmetric oscillator with piecewise-linearity, Chaos Solitons & Fractals 12 (2001) 1917–1927.
[18] T.Y. Li, J.A. Yorke, Period three implies chaos, American Math Monthly 82 (1975) 985–990.
[19] B.H. Tongue, K. Gu, Interpolated cell mapping of dynamical Systems, Journal of Applied Mechanics 55 (1988) 461–466.
[20] J. Guckenheimer, P. Holmes, Nonlinear Oscillation Dynamical Systems and Bifurcation of Vector Fields, Springer, New York, 1983.